ORIGINAL RESEARCH

Dysregulation of miR-103a Mediates Cigarette Smoking–induced Lipid-laden Macrophage Formation

Yin Zhu[1], Yohan Han[1], Sultan Almuntashiri[1,2], Saugata Dutta[1], Xiaoyun Wang[1], Caroline A. Owen[3], and Duo Zhang[1,4]

[1]Clinical and Experimental Therapeutics, College of Pharmacy, University of Georgia and Charlie Norwood Veterans Affairs Medical Center, Augusta, Georgia; [2]Department of Clinical Pharmacy, College of Pharmacy, University of Hail, Hail, Saudi Arabia; [3]Division of Pulmonary and Critical Care Medicine, Brigham and Women's Hospital, Harvard Medical School, Boston, Massachusetts; and [4]Department of Medicine, Medical College of Georgia, Augusta University, Augusta, Georgia

ORCID ID: 0000-0002-9900-740X (X.W.).

Abstract

Cigarette smoke (CS) is considered a major risk factor for chronic obstructive pulmonary disease (COPD) that is currently the third leading cause of death in the United States. Studies have indicated that patients with COPD have elevated blood low-density lipoprotein levels, which may contribute to the dysregulation of lipid metabolism. Accumulating data show that microRNAs (miRNAs) are involved in various human diseases. However, the role of microRNAs in the pathogenesis of COPD remains poorly defined. In this study, we found that miR-103a expression was significantly reduced in alveolar macrophages from smokers and patients with COPD versus that in alveolar macrophages from nonsmokers. Our data indicated that reactive oxygen species negatively regulate miR-103a in macrophages. Functionally, miR-103a modulates the expressions of genes involved in lipid metabolism and directly targets low-density lipoprotein receptors in macrophages. Furthermore, overexpression of miR-103a suppressed the accumulation of lipid droplets and reduced the reactive oxygen species, both *in vitro* and *in vivo*. Taken together, our findings indicate that downregulation of miR-103a contributes to cigarette smoke-induced lipid-laden macrophage formation and plays a critical role in lipid homeostasis in lung macrophages in the pathogenesis of COPD.

Keywords: small noncoding RNA; low-density lipoprotein receptor; chronic obstructive pulmonary disease; lipid-laden macrophages; oxidative stress

Cigarette smoke (CS) is the major risk factor for the development of chronic obstructive pulmonary disease (COPD), a respiratory disease hallmarked by airflow limitation because of airway mucosal inflammation, small airway remodeling, and destruction of the alveolar walls (emphysema) (1). COPD is a major global health problem and is currently the third leading cause of death worldwide (2). The disease affects both males and females, and the incidence increases with increasing age (3). Nearly half of patients with COPD remain undiagnosed as significant lung function can be lost before symptoms develop, and many patients only present to healthcare providers when their symptoms worsen and their quality of life is impaired (4).

Alveolar macrophages (AMs) serve as the "first-line defense" of the respiratory system and play a central role in lung diseases (5). The inflammatory response in the lung during the pathogenesis of COPD pathogenesis includes a significant increase in the number of AMs, mainly because of monocyte recruitment (6). In addition, the dysfunction of AMs caused by altered lipid metabolism has been linked to the pathogenesis of COPD (7).

Several studies have linked AMs to CS-induced altered metabolism of lipids, including surfactant proteins leading to alterations in macrophage function (8, 9).

(Received in original form May 13, 2022; accepted in final form September 2, 2022)

Supported by the National Institutes of Health (NIH) grants NIH/National Heart, Lung, and Blood Institute R00HL141685 (D.Z.), NIH/National Institute of Allergy and Infectious Diseases (NIAID) R03AI152003 (D.Z.), and NIH/NIAID R03AI169063 (X.W.).

Author Contributions: D.Z., Y.Z., and C.A.O. designed the research; Y.Z., D.Z., Y.H., S.D., and X.W. performed experiments; Y.Z., D.Z., S.A., and X.W. collected, analyzed, and interpreted data; and Y.Z., D.Z., and C.A.O. wrote the manuscript.

Correspondence and requests for reprints should be addressed to Duo Zhang, Ph.D., Clinical and Administrative Pharmacy, College of Pharmacy, University of Georgia, 1120 15th Street, HM Building, Augusta, GA 30912-2450. E-mail: duozhang@uga.edu.

This article has a related editorial.

This article has a data supplement, which is accessible from this issue's table of contents at www.atsjournals.org.

Am J Respir Cell Mol Biol Vol 67, Iss 6, pp 695–707, December 2022

Originally Published in Press as DOI: 10.1165/rcmb.2022-0202OC on September 6, 2022
Internet address: www.atsjournals.org

Type II alveolar epithelial cells produce surfactant proteins that maintain low surface tension and prevent alveolar collapse. CS exposure is associated with increased oxidative stress levels in the lungs, leading to oxidation of pulmonary surfactant (7–9). AMs normally ingest and degrade oxidized surfactants, but when exposed to CS, the processing of oxidized surfactants by AMs is dysfunctional, leading to the accumulation of lipids in AMs, which is a defining feature of lipid-laden macrophages or foam cells (5, 10). Another study reported that CS also altered the size of the AMs in patients with COPD and that while small macrophages are still highly phagocytic, larger, lipid-laden macrophages have lower proinflammatory and phagocytic functions (11). Together, these studies suggest that there is a direct link between CS exposure and dysregulation of lipid metabolism in AMs. However, the molecular mechanism by which CS exposure induces the formation of lipid-laden macrophages is unknown.

MicroRNAs (miRNAs) are a group of small noncoding RNAs with approximately 21–23 nucleotide molecules and serve as a pivotal regulator of various cellular processes, including proliferation, differentiation, and cell death (12, 13). Several research groups have shown that miRNAs are involved in the pathogenesis of COPD (14, 15). Among these studies, the downregulation of miR-103a has been linked to lung diseases, including non–small-cell lung cancer (10).

In the current study, we found that the expression of miR-103a was reduced in AMs from smokers and patients with COPD compared with that in AMs from nonsmokers. To further investigate these observations, we treated macrophages with cigarette smoke extract (CSE) *in vitro* and found that miR-103a was significantly downregulated. In addition, the downregulation of miR-103a caused by CSE exposure was rescued by adding NAC (N-acetylcysteine), an antioxidant, suggesting that oxidative stress contributes to the decrease in miR-103a expression in macrophages. TaqMan Array was performed using primary macrophages treated with a miR-103a mimic, a miR-103a inhibitor, or CSE to determine whether miR-103a is involved in the changes of lipid metabolism-associated genes. Our data indicated that the low-density lipoprotein receptor (LDLR) is a downstream target of miR-103a using both *in vitro* and *in vivo* models. Functionally, overexpression of miR-103a inhibited CSE- or oxidized LDL (oxiLDL)-induced lipid-laden macrophage formation and reduced reactive oxygen species (ROS) levels in macrophages *in vitro* and/or *in vivo*. Taken together, our study demonstrated that the reduced miR-103a expression induced by CS exposure drives the abnormal lipid accumulation in macrophages and that miR-103a may serve as a therapeutic target to reduce lipid-laden macrophage formation in smoke-exposed lungs.

Methods

Human Specimens

The human samples of this study were acquired and conducted as described previously (16). Two cohorts were included in this study: a BAL cohort and an immunostaining cohort. miR-103a expression in AMs from the BAL cohort was quantified by quantitative reverse transcription PCR (RT-qPCR). In this cohort, 6 nonsmokers, 11 smokers, and 8 patients with COPD were included (demographic and clinical characteristics are shown in Table 1), and all of them were recruited at Brigham and Women's Hospital. The BAL samples were collected, centrifuged, aliquoted, and stored at −80 °C (16). The double immunofluorescence staining of LDLR and CD68 was performed in lung sections from the immunostaining cohort, in which four nonsmokers and six patients with COPD were included (demographic and clinical characteristics are shown in Table 2). The lung sections in this cohort were provided by the LTRC (Lung Tissue Research Consortium) or the Department of Pathology at Brigham and Women's Hospital (16). Human studies were approved by the institutional review boards at Brigham and Women's Hospital (16).

Animal Studies

Wild-type C57BL/6 mice of both sexes (6- to 8-week-old) were purchased from the Jackson Laboratory. Under 2% isoflurane anesthesia condition, 25 μg oxiLDL (Thermo Fisher) in 50 μl Opti-MEM (Thermo Fisher) was first administered to the mice by oropharyngeal aspiration using a pipette and sterile tip (17). The mimic control and miR-103a mimic (200 pmol) were mixed with lipofectamine 2000 as described above. Thirty minutes after oxiLDL treatment, mimic control and miR-103a mimic-loaded liposomes (200 pmol in 50 μl Opti-MEM) were delivered via oropharyngeal aspiration. Next, the primary AMs were isolated from BAL fluid according to the described method (18) after 48 hours. Cytocentrifuge preparations of the AMs were fixed with 10% formalin in saline (Sigma-Aldrich) and then prepared for staining with LipidTOX dye (Invitrogen) or Oil Red O (ORO) dye (Sigma-Aldrich). All the animal studies were approved by the Charlie Norwood Veterans Affairs Medical Center Institutional Animal Care and Use Committee and followed the ARRIVE guideline (Animal Research: Reporting of In Vivo Experiments).

The CS exposure method was performed as described previously (16). All the animal studies were approved by Institutional Care and Use Committee at Brigham and Women's Hospital. Briefly, wild-type mice in the CS group were exposed to mixed main-stream and side-stream CS from 3R4F research cigarettes (University of Kentucky) for 2 hours per day and 6 days per week in chambers, whereas the room air control group was exposed only to room air. Lung tissues were harvested, fixed in formalin, and then embedded in paraffin for subsequent analysis.

Additional Methods

Additional experimental details and methods are provided in the data supplement.

Results

CS Exposure Decreases miR-103a Expression in Macrophages

miR-103a has been proposed as a potential therapeutic target for lung cancer (19), but its regulation and function have not been studied in COPD. As shown in Figure E1A in the data supplement, analysis of data from the FANTOM5 (Functional ANnoTation Of Mammalian Genome) database revealed that miR-103a is expressed by diverse cell types but is most highly expressed by human myeloid leukocytes, including macrophages, polymorphonuclear leukocytes, monocytes, and dendritic cells (20). In addition to human primary cells, we measured miR-103a expression levels in various murine tissues. miR-103a is detectable in multiple tissues and is highly expressed in murine lung and brain (Figure E1B). We next compared miR-103a expression levels in AMs in the BAL cohort including nonsmokers ($n = 6$), smokers

Table 1. Bronchoalveolar Lavage Cohort: Demographic and Clinical Characteristics

Characteristics	Nonsmokers* ($n=6$)	Smokers† ($n=11$)	Patients with COPD‡ ($n=8$)	*P* Value§
Males, *n* (%)	5 (83)	7 (36)	3 (38)	$P=0.2113$
Age, yr	59 ± 10	65 ± 5	68 ± 5	$P=0.1536$
Pack-years of smoking	0	38 (12–68)	34 (7–160)	$P=0.001$‖
Number of current smokers, *n* (%)†	0 (0)	0 (0)	5 (63)	$P=0.0013$
FEV_1% predicted	94 ± 8	91 ± 11	69 ± 22	$P=0.006$¶
FEV_1/FVC% predicted	77 ± 3	78 ± 3	56 ± 12	$P<0.001$**

Definition of abbreviations: COPD = chronic obstructive pulmonary disease; FEV_1 = forced expiratory volume in 1 second; FVC = forced vital capacity.

The table shows the demographic and clinical characteristics of the patients with COPD, smokers without COPD, and nonsmoker control subjects who underwent BAL as part of another research study (16). Data are presented as median (interquartile range) for data that were not normally distributed or mean ± SD for data that were normally distributed.

*Nonsmokers were all never-smokers.

†Smokers were defined as subjects who had 10 pack-years or more of smoking history. Current smokers were defined as active smokers at the time of the bronchoscopy or had stopped smoking less than 1 year before the bronchoscopy was performed.

‡All patients with COPD had $FEV_1/FCV < 0.7$, whereas smokers without COPD and nonsmoker control subjects had $FEV_1/FCV \geq 0.7$.

§Categorical variables were analyzed with a chi-square test. Statistical analyses included one-way ANOVA tests for continuous variables (age, FEV_1% predicted, FEV_1/FCV, and pack-years of smoking history) followed by pairwise comparisons using two-tailed Student's *t* tests for data that were normally distributed or Mann-Whitney *U* tests for data that were not normally distributed.

‖The pack-years of smoking histories of the patients with COPD were not significantly different from those of the smokers ($P=0.408$). The pack-years of smoking histories of the patients with COPD and the smokers were significantly different from those of the nonsmoker group by design ($P<0.001$ for both comparisons).

¶The FEV_1 values for the patients with COPD were significantly lower than those of the smokers ($P=0.011$) and nonsmokers by design ($P=0.023$). The FEV_1 values for the smokers were not significantly different from those for the nonsmoker groups ($P=0.598$).

**The FEV_1/FVC ratios for the patients with COPD were significantly lower than those of the smoker and nonsmoker groups by design ($P<0.001$ for both comparisons). The FEV_1/FVC ratios of the smokers were not significantly different from those of the nonsmokers ($P=0.909$).

($n=11$), and patients with COPD ($n=8$). The demographic and clinical characteristics of this cohort are listed in Table 1. Our results showed that the expression of miR-103a was significantly lower in AMs from smokers and patients with COPD than in AMs from nonsmokers (Figure 1A) ($P=0.0174$ and $P=0.0345$ vs. nonsmokers, respectively). We next evaluated the *in vitro* effects of smoke exposure on miR-103a expression in macrophages. Before that, we tested various CSE concentrations and found that 5–15% CSE treatment for 12 hours did not affect THP-1 cell viability (Figure 1B). Results produced by RT-qPCR show that treatment of CSE from 5% to 15% can reduce the miR-103a level in THP-1 macrophages (Figure 1C). Notably, both 10% and 15% CSE

Table 2. Lung Immunostaining Cohort: Demographic and Clinical Characteristics

Characteristics	Nonsmokers* ($n=4$)	Patients with COPD† ($n=6$)	*P* Value‡
Males, *n* (%)	2 (50)	3 (50)	$P>0.9999$
Age, yr	52 ± 8	60 ± 5	$P=0.165$
Pack-years of smoking	0	45 ± 20	$P=0.002$§
Current smokers, *n* (%)‖	0 (0)	0 (0)	$P>0.9999$
FEV_1% predicted	102 ± 18	26 ± 12	$P<0.001$¶
FEV_1/FVC % predicted	81 (74–104)	37 (32–51)	$P=0.01$**

The table shows the demographic and clinical characteristics of the patients with chronic obstructive pulmonary disease (COPD), smokers without COPD, and nonsmoker control subjects who underwent either a lung biopsy, lung volume reduction surgery, or lung transplantation. Data are presented as median (interquartile range) for data that were not normally distributed or mean ± SD for data that were normally distributed.

*Nonsmokers were all never-smokers.

†All patients with COPD had $FEV_1/FCV < 0.7$, whereas nonsmoker control subjects had $FEV_1/FCV \geq 0.7$.

‡Categorical variables were analyzed with a chi-square test. Statistical analyses included one-way ANOVA tests for continuous variables (age, FEV_1% predicted, FEV_1/FCV, and pack-years of smoking history) followed by pairwise comparisons using two-tailed Student's *t* tests for data that were normally distributed or Mann-Whitney *U* tests for data that were not normally distributed.

§The pack-years of smoking histories of the patients with COPD were significantly different from those of the nonsmoker group by design ($P=0.002$).

‖Current smokers were defined as active smokers at the time the samples were obtained or had stopped smoking less than 1 year before the samples were obtained.

¶The FEV_1 values for the patients with COPD were significantly lower than those of the nonsmokers by design ($P<0.001$).

**The FEV_1/FVC ratios for the patients with COPD were significantly lower than those of the nonsmoker groups by design ($P=0.01$).

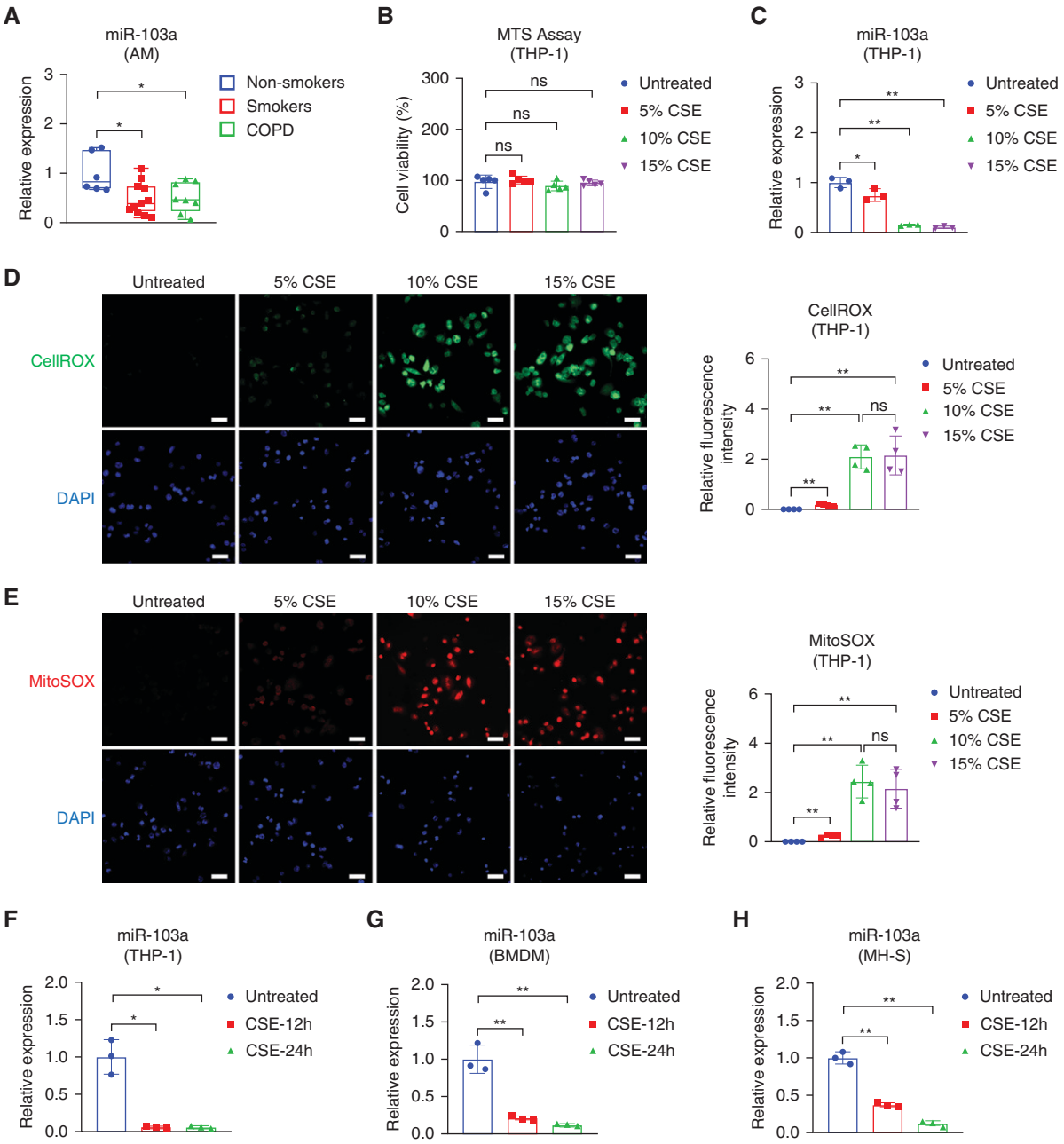

Figure 1. Cigarette smoke exposure decreases miR-103a expression in macrophages. (*A*) Relative expression of miR-103a in alveolar macrophages (AMs) in nonsmokers ($n = 6$), smokers ($n = 11$) and patients with chronic obstructive pulmonary disease (COPD) ($n = 8$) measured by reverse transcription quantitative PCR (RT-qPCR). (*B*) THP-1 cells were cultured with 5%, 10%, and 15% cigarette smoke extract (CSE) for 12 hours. Cell viability was analyzed using an MTS assay. (*C*) miR-103a levels was measured in THP-1 cells cultured with 5%, 10%, and 15% CSE for 12 hours. (*D* and *E*) THP-1 cells were cultured with 5%, 10%, and 15% CSE for 12 hours. One μM CellROX dye or 5 μM MitoSOX red dye was added to detect the (*D*) cellular and (*E*) mitochondrial reactive oxygen species (ROS) levels. The nucleus was stained with DAPI. The images were taken using a fluorescence microscope, and the intensity was quantified by ImageJ software. Scale bar, 100 μm. (*F–H*) Cells were cultured with 10% CSE for 12 and 24 hours. miR-103a expression was detected in (*F*) THP-1, (*G*) bone marrow-derived macrophage (BMDM), and (*H*) MH-S cells using RT-qPCR. The data were from 3–5 independent experiments. $P > 0.05$, $^{*}P < 0.05$, and $^{**}P < 0.01$. MTS = [3-(4,5-dimethylthiazol-2-yl)-5-(3-carboxymethoxyphenyl)-2-(4-sulfophenyl)-2H-tetrazolium]; ns = not significant.

treatment strikingly downregulated miR-103a expression (Figure 1C). It is well known that CSE contains large amounts of unstable free radicals, which enhance ROS production (21). Therefore, we confirmed the cellular and mitochondrial ROS levels in these CSE-treated THP-1 cells. We observed that both were significantly induced by CSE, especially at 10% and 15% (Figures 1D and 1E). In addition to the dose–response, using the THP-1 cells, murine bone marrow-derived macrophage (BMDM), and MH-S cells, we demonstrated a

similar pattern of miR-103a expression reduced by 10% CSE at both 12 and 24 hours (Figures 1F–1H).

Oxidative Stress Mediates CSE-induced Downregulation of miR-103a

To further determine the contribution of oxidative stress in CS-induced miR-103a downregulation in macrophages, macrophages were preincubated with a general ROS inhibitor NAC (N-acetylcysteine) or a mitochondrial antioxidant Mito-TEMPO and then treated with CSE. The CSE-induced reduction in miR-103a expression was significantly rescued by adding NAC in THP-1 cells but not altered by adding Mito-TEMPO (Figure E2A). Consistently, the CSE-reduced miR-103a levels were also attenuated by NAC in MH-S (Figure E2B) and BMDM cells (Figure E2C). Treating these cells with H_2O_2 also decreased miR-103a expression, and NAC pretreatment rescued H_2O_2-induced suppression of miR-103a expression in THP-1 (Figure E2D) and MH-S cells (Figure E2E). Taken together, our data suggested that the oxidative stress associated with CSE is at least in part responsible for the CSE-induced downregulation of miR-103a observed in macrophages.

miR-103a Regulates Genes Involved in Lipid Metabolism

Previous studies have revealed that CS exposure causes the alteration of lipid metabolism in the lung (5, 22). To test whether miR-103a mediates the dysregulation of lipid metabolism during CS exposure, lipid-regulated genes were examined in BMDM using TaqMan Array (Table E1). The expression of miR-103a was measured after miR-103a overexpression (Figure 2A), inhibition (Figure 2B), or CSE treatment (Figure 2C). We found that multiple lipid-regulated genes were robustly altered by overexpression (Figure 2D), inhibition (Figure 2E), or CSE treatment (Figure 2F). Among the screened genes, we observed that the expression of Cox2 (Ptgs2) and Ldlr were consistently altered (Figure 2G). Next, we validated the data using RT-qPCR and observed that miR-103a significantly reduced Ldlr expression. However, miR-103a overexpression did not change Cox2 expression in BMDM (Figure 2H). Our data suggested that miR-103a may participate in the alteration of lipid metabolism in macrophages induced by CS exposure.

CS Exposure Promotes LDLR Expression in Lung Macrophages

Poliska and colleagues compared gene expression in AMs and circulating monocytes between patients with COPD and healthy control subjects (23). We found that steady-state LDLR mRNA levels were significantly increased in AMs from patients with COPD compared with those from the control group (Figure 3A). Similarly, increased LDLR expression was detected in peripheral blood monocytes (Figure 3B) but not in peripheral blood mononuclear cells (PBMCs) (Figure 3C) (GEO accession: GSE42057) (6), which are likely to be predominantly lymphocytes. Next, we examined LDLR levels in lung macrophages from patients with COPD versus control subjects in the lung immunostaining cohort by double immunostaining the lung sections for LDLR and a marker of macrophages (CD68). The demographic and clinical characteristics of the lung immunostaining cohort are shown in Table 2. LDLR staining was significantly greater in lung macrophages in patients with COPD ($n = 6$) compared with nonsmokers ($n = 4$) (Figure 3D) ($P = 0.0256$). Consistent with these results, significantly increased LDLR immunostaining was detected in macrophages in lung sections from mice exposed to CS versus air for 6 months (Figure E3). Upregulation of LDLR was confirmed at the protein level in primary AMs after 5% CSE treatment using immunofluorescence staining (Figure 3E). Results produced by flow cytometry analysis using AMs from mice exposed to CS versus air for 6 months were similar to those obtained by immunofluorescence staining (Figure 3F). Together, these data indicate that patients with COPD have elevated macrophage LDLR levels and that CS exposure increases LDLR expression on macrophages.

LDLR Is a Direct Target of miR-103a

As miR-103a overexpression decreased Ldlr at the mRNA degree in BMDM, we transfected miR-103a mimic or mimic control into BMDM and THP-1 cells and then exposed them to CSE. The overexpression of miR-103a in BMDM and THP-1 cells was confirmed (Figures E4A and E4B). Western blot analysis showed that LDLR protein levels were reduced by the miR-103a mimic in both cell types (Figures 4A and 4B). Similar results were obtained in 5% CSE-treated primary AMs using immunofluorescence staining (Figure 4C) after miR-103a overexpression (Figure E4C). To further test if LDLR is a direct target of miR-103a, the 3′-untranslated region (UTR) of LDLR containing the potential miR-103a binding sites was subcloned into a pRL-TK luciferase reporter vector (Figure 4D). Luciferase assays demonstrated that miR-103a mimic transfection repressed luciferase activity via the LDLR 3′-UTR. The inhibitory effect of miR-103a was lost when the miR-103a binding site in the reporter vector was mutated (Figure 4E). These results indicated that LDLR is a direct target of miR-103a in macrophages.

Lipid-laden Macrophage Formation Is Suppressed by miR-103a

It has been reported that the size of AMs is significantly increased in patients with COPD, and this is also a characteristic of lipid-laden macrophages (24, 25). As shown in Figure E5A, $CD68^+$ lung macrophages from mice exposed to CS for 6 months were larger than those from the air control group. To determine whether CSE exposure increases macrophage size by increasing intracellular lipid accumulations, THP-1 cells were treated with CSE and stained with ORO. Lipid droplet formation was observed after 5% CSE treatment for 4 days (Figure E5B). Interestingly, we found that lipid accumulation induced by 5% CSE for 4 days was suppressed by miR-103a overexpression (Figure 5A). Next, we assessed whether miR-103a reduces lipid accumulation in macrophages *in vivo*. As shown in Figure 5B, oxiLDL was given to the mice via oropharyngeal aspiration to induce lipid-laden macrophages. Thirty minutes after oxiLDL administration, miR-103a mimic or a mimic control was delivered to the mice. The relative expression levels of miR-103a and Ldlr in AMs collected from BAL were measured using RT-qPCR (Figures E6A and E6B). The percentage of ORO-positive AMs was significantly decreased in the miR-103a mimic treated group (Figure 5C). Furthermore, the LipidTOX staining confirmed that miR-103a overexpression suppresses oxiLDL-induced lipid droplet formation in the AMs (Figure 5D). Thus, our data suggested that miR-103a plays a role in lipid-laden macrophage formation.

To determine whether LDLR mediates the role of miR-103a in lipid-laden macrophage formation, we performed a

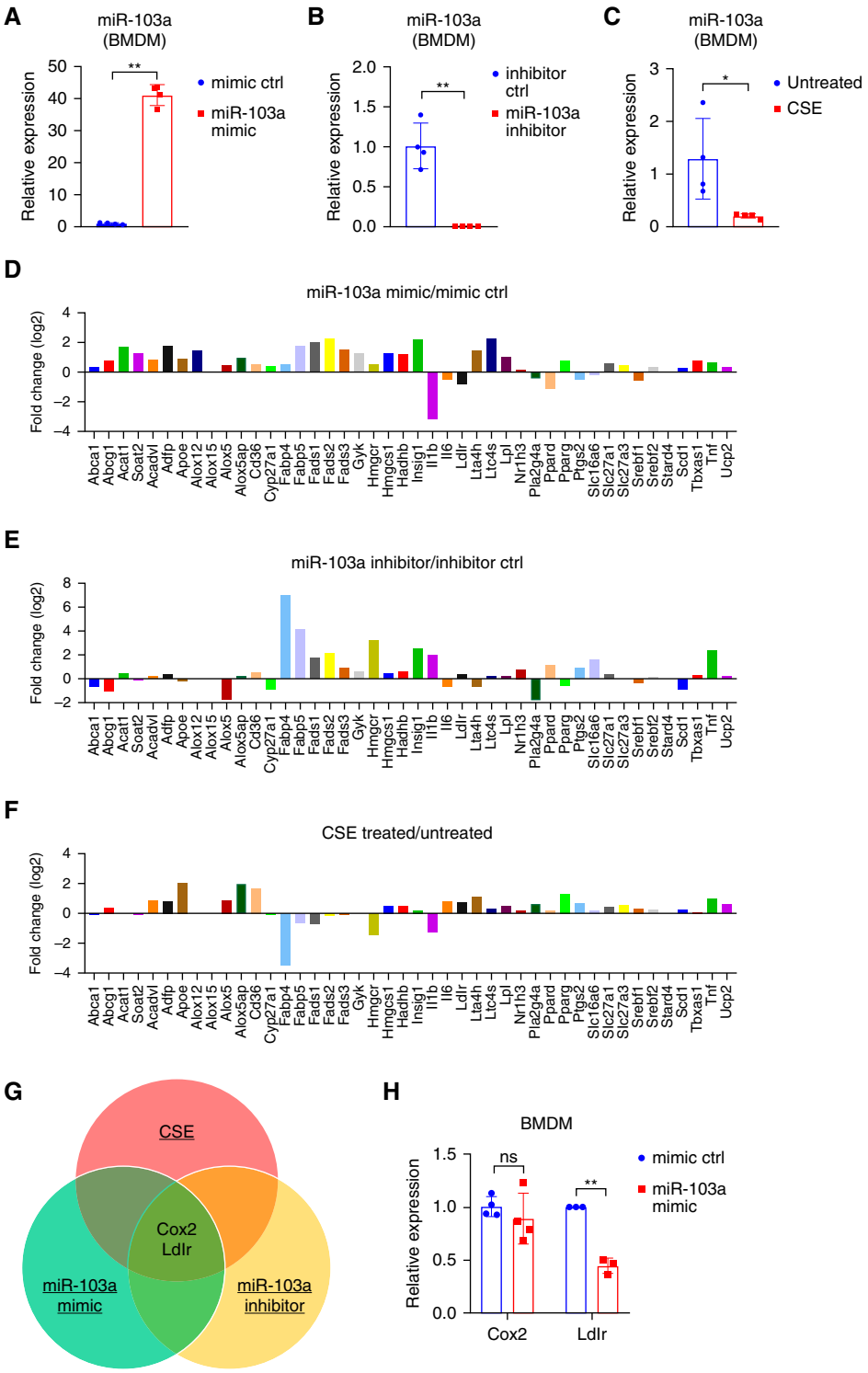

Figure 2. Cigarette smoke (CS) regulates genes involved in lipid metabolism in macrophages *via* miR-103a. (*A–G*) BMDM (pooled RNA from four independent experiments) were transfected with (*A* and *D*) miR-103a mimic/mimic control, (*B* and *E*) miR-103a inhibitor/inhibitor control, or (*C* and *F*) treated with 10% CSE. (*A–C*) Forty-eight hours after transfection or treatment, miR-103a expression levels were measured using RT-qPCR. Taqman array was performed to detect genes involved in lipid metabolism. (*D–F*) The fold change was normalized to the control group, and log2 transformed, respectively. (*G*) Venn diagram showing the genes with consistent changes in response to miR-103a overexpression, inhibition, and CSE treatment. (*H*) BMDM were transfected with miR-103a mimic or mimic control. Forty-eight hours after transfection, the mRNA expression of Cox2 and Ldlr in BMDM was detected using qRT-PCR. The data were from 4 independent experiments. $P > 0.05$ and $^{**}P < 0.01$. ctrl = control.

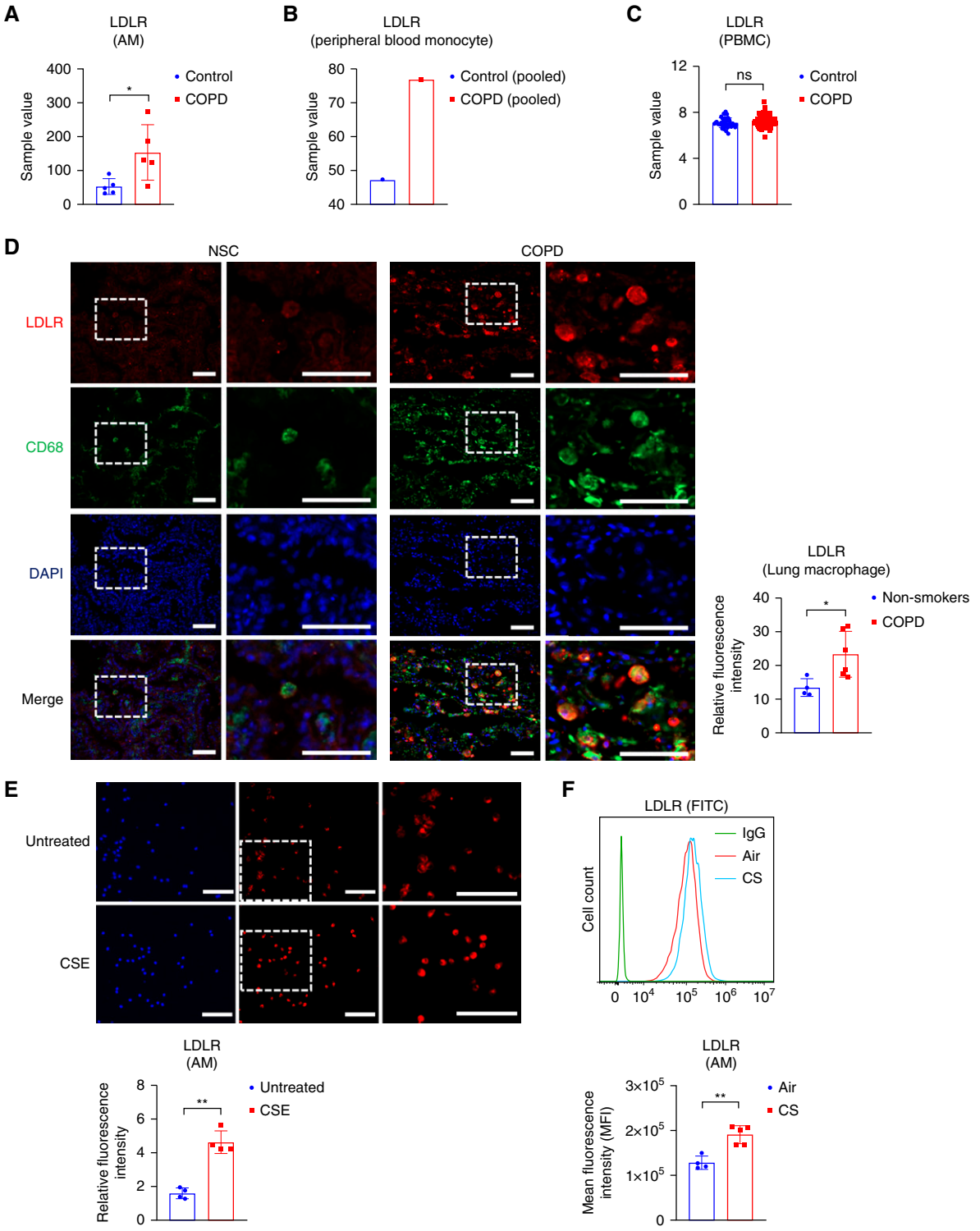

Figure 3. Cigarette smoke (CS) exposure induces low-density lipoprotein receptor (LDLR) in lung macrophages. (*A–C*) Analysis of LDLR expression using Gene Expression Omnibus (GEO) dataset. (*A*) LDLR sample values in AMs from patients with chronic obstructive pulmonary disease (COPD) ($n = 6$) and control subjects ($n = 6$). (*B*) LDLR sample value in pooled peripheral blood monocytes from patients with COPD ($n = 5$) and control subjects ($n = 5$). (*C*) LDLR sample value in PBMCs from patients with COPD ($n = 92$) and control subjects ($n = 42$). (*D*) Antibodies against LDLR and CD68 were used to conduct immunofluorescence staining in lung sections of patients with COPD ($n = 6$) and nonsmoker control subjects ($n = 4$). Scale bar, 50 μm. (*E*) The AMs were treated with or without 5% CSE for 12 hours. LDLR immunofluorescence staining was performed. Scale bar, 50 μm. (*F*) Mice were exposed to CS or room air for 6 months. The LDLR protein levels in AMs were compared in the air group ($n = 4$) and CS-exposed group ($n = 5$) using flow cytometry. $P > 0.05$, $^*P < 0.05$, and $^{**}P < 0.01$. FITC = fluorescein isothiocyanate; IgG = immunoglobulin G; PBMC = peripheral blood mononuclear cell.

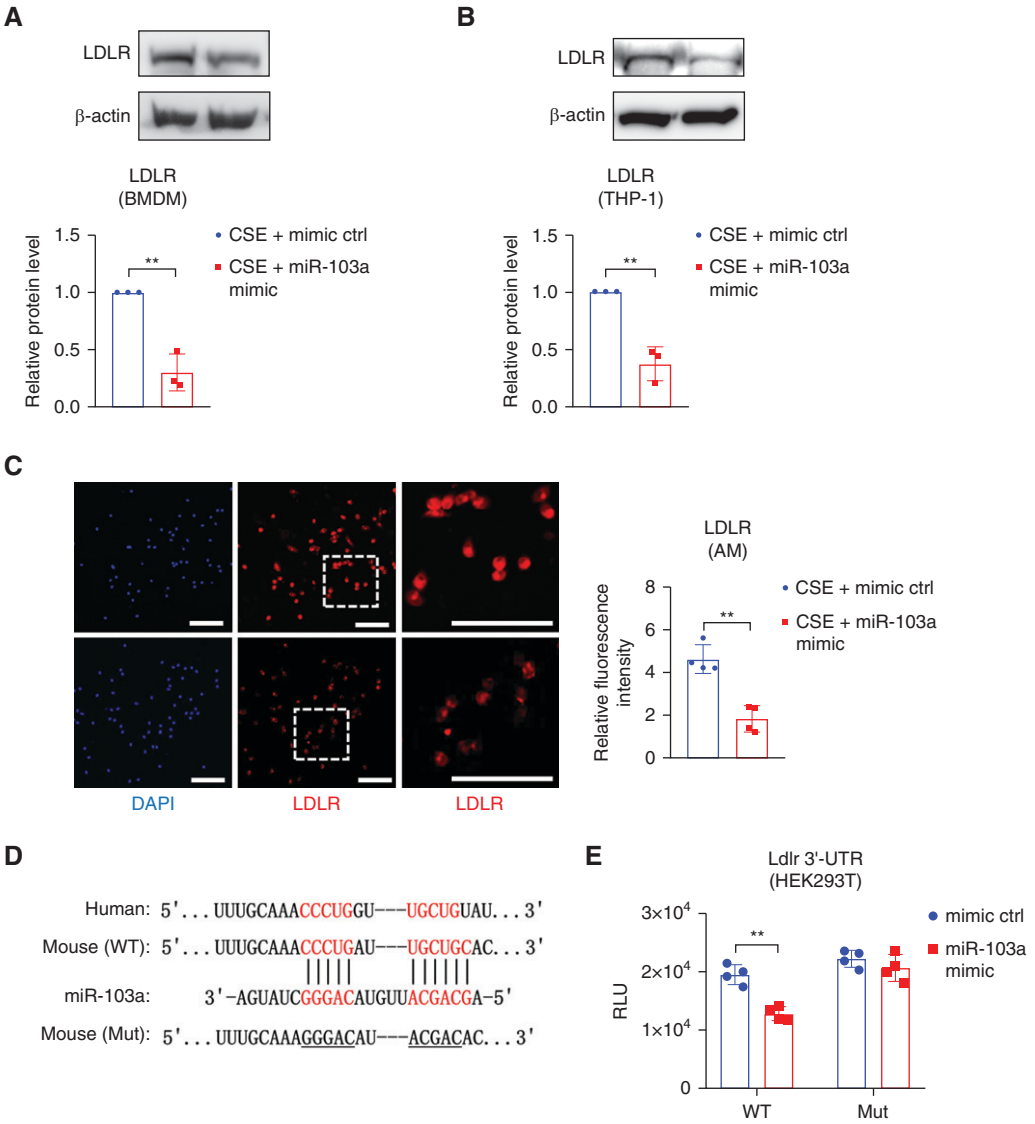

Figure 4. miR-103a directly targets LDLR in macrophages. (*A* and *B*) Cells incubated with 10% CSE were transfected with the miR-103a mimic or mimic control. After 48 hours, the LDLR protein level was detected in (*A*) BMDM and (*B*) THP-1 using Western blot. (*C*) AMs incubated with 5% CSE were transfected with the miR-103a mimic or mimic control. After 48 hours, the LDLR protein level was detected using immunofluorescence staining. Scale bar, 50 μm. (*D*) The sequence of the potential miR-103a binding site in the LDLR 3′-untranslated region (UTR). (*E*) Renilla luciferase reporter containing WT or Mut Ldlr 3′-UTR was cotransfected with miR-103a mimic or mimic control to HEK293T cells. Luciferase assay was performed 48 hours after transfection. $^{**}P < 0.01$. Mut = mutant; RLU = relative luminescence units; WT = wild type.

rescue experiment. First, transfection was confirmed in RAW 264.7 macrophages (Figures E7A and E7B). As shown in Figure E7C, overexpressing LDLR using *LDLR* coding sequence without the 3′-UTR significantly attenuated the effect of miR-103a on CSE-induced lipid accumulation.

Overexpression of miR-103a Reduces ROS Levels in Macrophages

Oxidative stress is a key effector pathway in the immune response and fundamental in pathogen killing by macrophages (5, 26). As oxidative stress reduces miR-103a expression in macrophages, we assessed whether changes in miR-103a expression, in turn, alter oxidative stress levels in macrophages, thus creating a vicious cycle. In CSE-treated THP-1 cells, both cellular and mitochondrial ROS levels were significantly reduced by miR-103a mimic transfection as indicated by staining cells with MitoSOX and CellROX dye (Figures 6A and 6B). In contrast, untreated cells contained much lower ROS than CSE-treated cells, and miR-103a did not alter cellular or mitochondrial ROS at the basal level (Figures 6A and 6B). Transfecting cells with miR-103a also reduced cellular and mitochondrial ROS levels in oxiLDL-treated AMs but not in the untreated group (Figures 6C and 6D). Our data indicate that miR-103a modulates macrophage ROS generation.

Discussion

COPD will remain a major worldwide health problem for the foreseeable future. Although some nonpharmacologic-based treatments

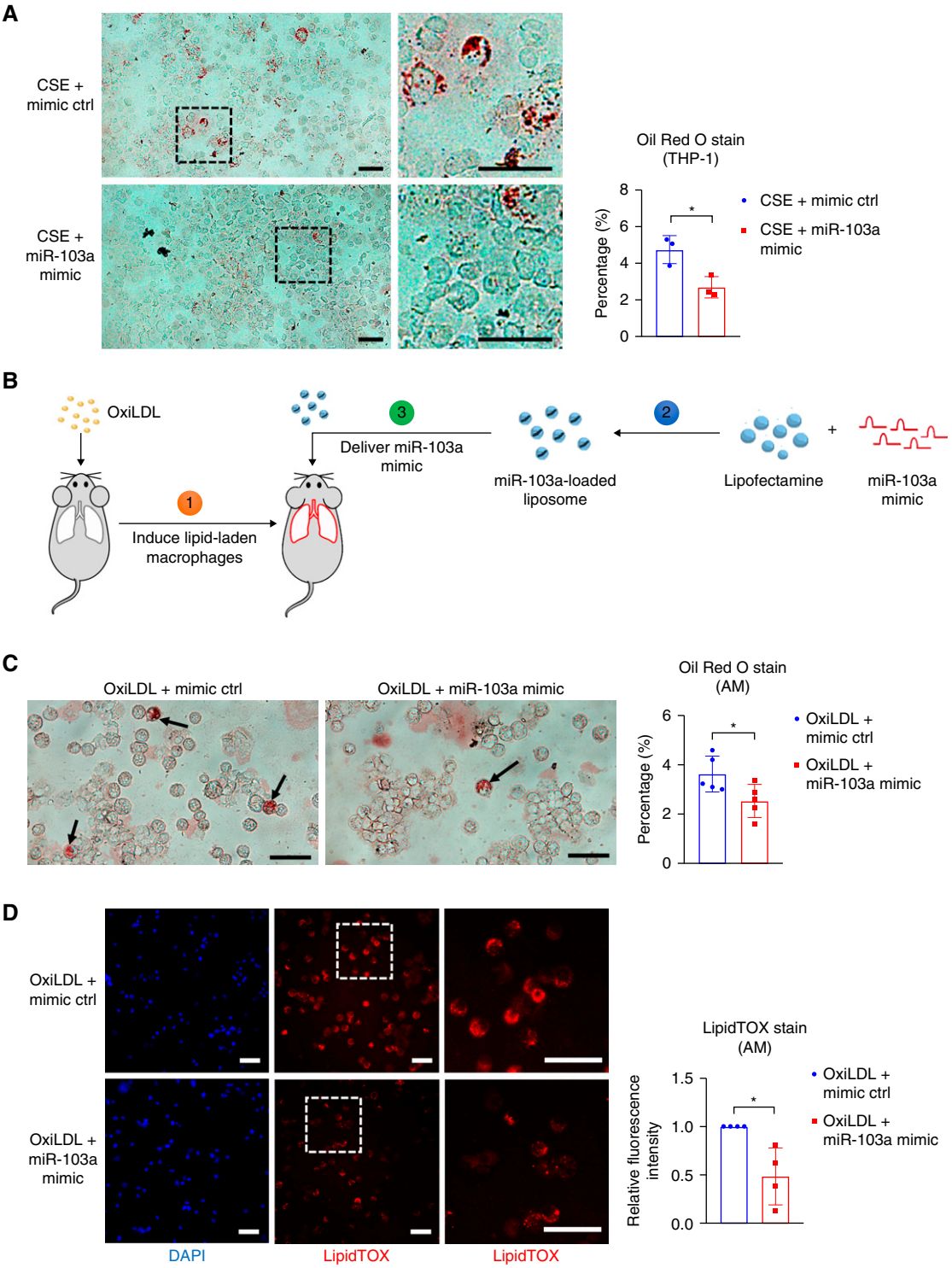

Figure 5. miR-103a overexpression suppresses lipid-laden macrophage formation. (*A*) THP-1 cells incubated with 5% CSE were transfected with miR-103a mimic or mimic control. ORO staining was performed 4 days after transfection. Scale bar, 50 μm. (*B–D*) Mice were given 50 ul Opti-MEM containing 25 μg oxiLDL *via* aspiration. (*B*) After 30 minutes, oxiLDL-treated mice were given 50 μl Opti-MEM containing 200 pmol miR-103a mimic or mimic control *via* aspiration. Schematic illustration of delivering the miR-103a mimic or mimic control to oxiLDL-treated mice. (*C*) AMs were isolated at 48 hours after the treatment, and the lipid-laden macrophage formation was assessed by ORO staining ($n = 5$ per group) and (*D*) LipidTOX dye staining ($n = 4$ per group). $^*P < 0.05$. LDL = low-density lipoprotein; ORO = Oil Red O.

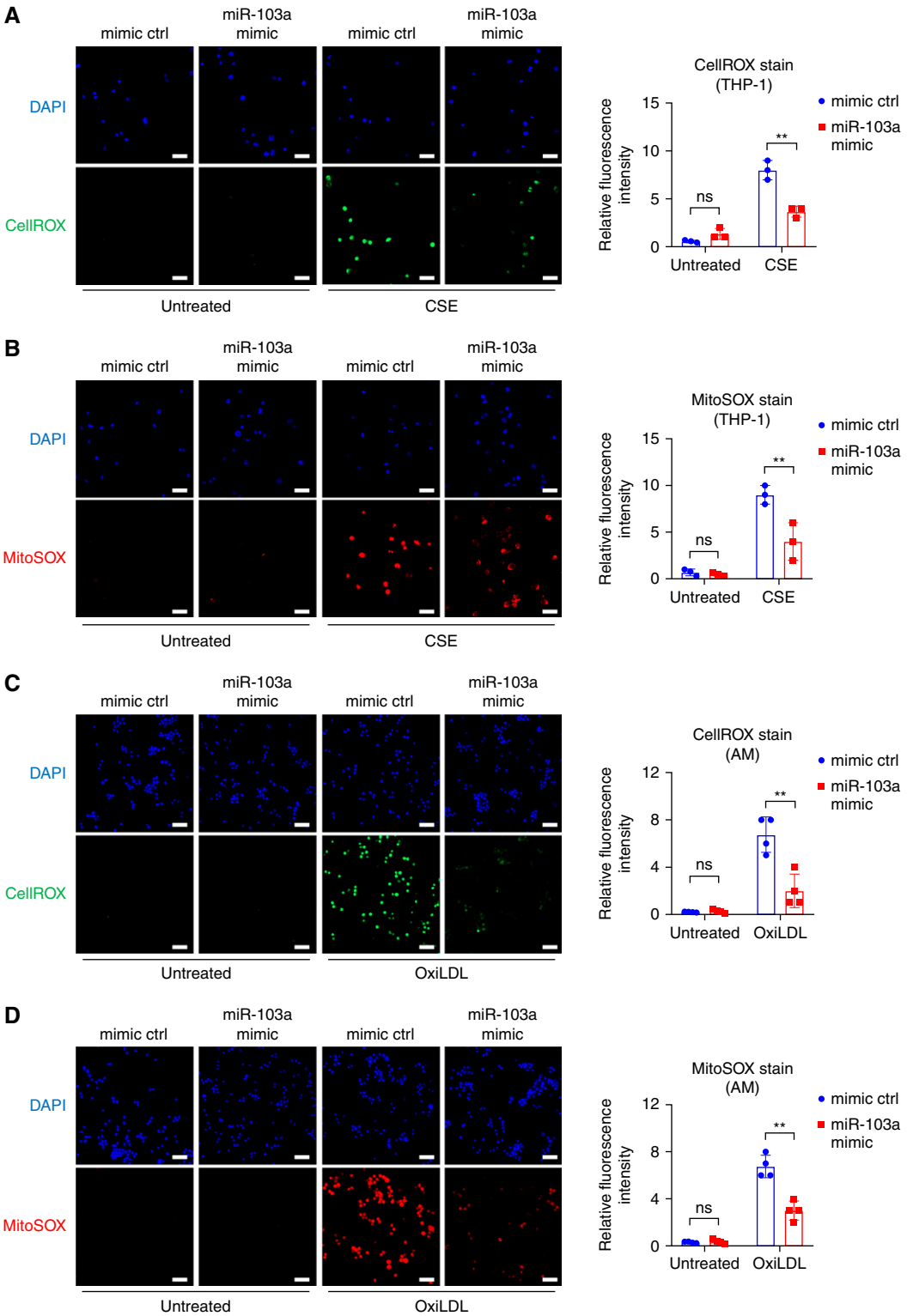

Figure 6. miR-103a overexpression reduces reactive oxygen species (ROS) generation in macrophages. (*A* and *B*) THP-1 cells incubated with or without 10% CSE were transfected with miR-103a mimic or mimic control. Forty-eight hours after transfection, (*A*) cellular and (*B*) mitochondrial ROS levels were detected using 1 μM CellROX dye or 5 μM MitoSOX red dye, respectively. DAPI was used to stain the cell nuclei. The images were taken usinga fluorescence microscope, and the intensity was quantified by ImageJ software. Scale bar, 100 μm. (*C* and *D*). Mice were given 50 μl Opti-MEM or 50 μl Opti-MEM containing 25 μg oxiLDL *via* aspiration. After 30 minutes, mice were given 50 μl Opti-MEM containing 200 pmol miR-103a mimic or mimic control *via* aspiration. AMs were isolated at 48 hours after the treatment, and ROS production was assessed by (*C*) CellROX staining ($n = 4$ per group) and (*D*) MitoSOX staining ($n = 4$ per group). $P > 0.05$ and $^{**}P < 0.01$.

for COPD, including smoking cessation and increasing physical activity, reduce exacerbation and mortality rates in patients with COPD, COPD is still associated with high morbidity and mortality (27, 28). No medical therapies exist that significantly alter the course of COPD or eliminate symptoms associated with this disease. Immune cells, including AMs, are considered sentinel in protecting the lung from inhaled noxious particles. However, in patients with COPD, smoke-induced increases in lung macrophage numbers and/or impairment in macrophage function have been linked to the worsening of the disease (29). Many studies have reported that exposure of AMs to CS leads to changes in macrophage characteristics and function, including increases in their size and impairment in their intracellular lipid metabolism (30). However, the mechanisms involved and the potential for new therapeutics targeting CS-induced macrophage dysfunction have not been well studied.

Robust expression of miR-103a has been reported in cells of myeloid origin, including macrophages, indicating a high potential for miR-103a to regulate macrophage cellular function (20). The regulation and function of miR-103a in various cancers, including non–small cell lung cancer, colorectal cancer, and gastric cancer, have been studied previously (19, 31, 32), but the contribution of miR-103a to the pathogenesis of COPD has not been evaluated. Our study is the first to explore the contribution of miR-103a to CS-induced dysregulated lipid accumulation in macrophages, a key cellular culprit in the pathogenesis of COPD. We showed that miR-103a expression is downregulated in AMs from both patients with spirometrically-confirmed COPD and smokers and also in macrophages exposed to CSE *in vitro*.

We identified *Ldlr* and *Cox2* genes as potential targets of miR-103a using TaqMan Array (Figure 3). In addition, miR-103a overexpression decreased Ldlr expression levels in macrophages as detected by RT-qPCR but does not alter Cox2 expression. Our findings show that LDLR expression levels are increased in lung macrophages from patients with COPD and are consistent with those reported previously by Poliska and colleagues (23). Intriguingly, our analysis of gene expression data from Poliska and colleagues that are in the public domain showed that LDLR expression levels are elevated in peripheral blood monocyte (pooled RNA samples, $n = 5$) from patients with COPD versus control subjects (GEO: GSE16972) (23). However, a GEO analysis of gene expression in PBMC reported no significant difference in LDLR expression between control subjects and COPD subjects (GEO: GSE42057). Peripheral blood monocytes represent only a minor (10–20%) subpopulation of leukocytes in PBMCs, and it is possible that an increased LDLR gene expression signal in the monocyte subpopulation was diluted out by the lymphocytes (representing 70–90% of all PBMCs) (33). A strength of our study is that we also showed that LDLR is induced by CSE treatment in primary AMs (Figure 3E). Similarly, LDLR is elevated in lung macrophages from CS-exposed mice versus those from the air group (Figures 3F and E3). Thus, the downregulation of miR-103a is more prominent in AMs than PBMCs, and the expression of miR-103a is negatively related to LDLR level in AMs.

A novel finding of our study is that miR-103a is a key negative regulator of LDLR expression in macrophages as CS-induced increases in LDLR protein levels were decreased by miR-103a overexpression in three different macrophages (BMDMs, THP-1 cells, and murine AMs). LDLR 3′-UTR luciferase reporter assays confirmed that miR-103a directly targets LDLR. Furthermore, we validated that LDLR mediates the effect of miR-103a in macrophages using a rescue experiment (Figure E7).

Another novel finding in our study is that miR-103a inhibits lipid accumulation in lung macrophages. An increase in LDLR levels in AMs from smokers and patients with COPD was observed in several studies (GEO: GSE16972 and GEO: GSE42057). Meanwhile, an increase in the size of lung macrophages has also been reported in smokers and patients with COPD, suggesting that large, lipid-laden macrophages accumulate in CS-exposed lungs. Although studies have suggested that lipid uptake in macrophages is mediated via scavenger receptors rather than LDL receptors, the role of the former in lipid-laden macrophage formation has been debated (34–36). Deletion of the scavenger receptor A and CD36 (receptors known to internalize LDL) did not efficiently decrease the formation of foam cells in an atherosclerosis murine model (34). To investigate the potential contributions of LDLR to the formation of lipid-laden macrophages, we performed ORO staining on CSE-treated macrophages. CSE treatment of macrophages significantly increased the number of ORO-positive macrophages, suggesting that CS induces the expression of LDLR in lung macrophages to thereby promote the formation of lipid-laden macrophages. As overexpression of miR-103a reduced LDLR expression in macrophages, we next studied the contributions of miR-103a to lipid-laden macrophage formation. There were fewer ORO-positive cells in the group treated with the miR-103a mimic than in the mimic control. When C57BL/6J mice were challenged with inhaled oxiLDL and treated with either the miR-103a or the control mimic, there were fewer ORO-positive alveolar macrophages in the miR-103a mimic-treated group. This result was confirmed when LipidTOX was used to stain the macrophages for intracellular lipids. Therefore, approaches to delivering miR-103a to the lungs may have therapeutic potential in COPD by reducing the formation of lipid-laden macrophages induced by inhaling CS.

CS contains large numbers of ROS and also increases lung oxidative stress levels by inducing the production of ROS by macrophages and other cells in the lung (37). Oxidative stress contributes to the pathogenesis of COPD (2). Our study showed that oxidative stress downregulates miR-103a expression as both CSE- and H_2O_2-treated cells have reduced expression of miR-103a, which was, in part, rescued by the antioxidant NAC but not Mito-TEMPO (Figure E2). Another intriguing finding in our study is that mitochondrial and cellular ROS levels were attenuated by overexpressing miR-103a. Previous findings in endothelial cells showed that H_2O_2 treatment significantly decreases the expression of miR-103 in human umbilical vein endothelial cells (38). Overexpression of miR-103 reduces H_2O_2-induced ROS production (38). Another study demonstrated that miR-103a alleviates lipopolysaccharide-induced oxidative stress in BV2 glial cells by targeting HMGB1 (39). Nevertheless, little is known about the molecular interactions between ROS and miR-103a, particularly in macrophages. Further investigations are needed to address the knowledge gap. In our study, elevated levels of oxidative stress caused by CS exposure downregulate the expression of miR-103a in macrophages, leading to

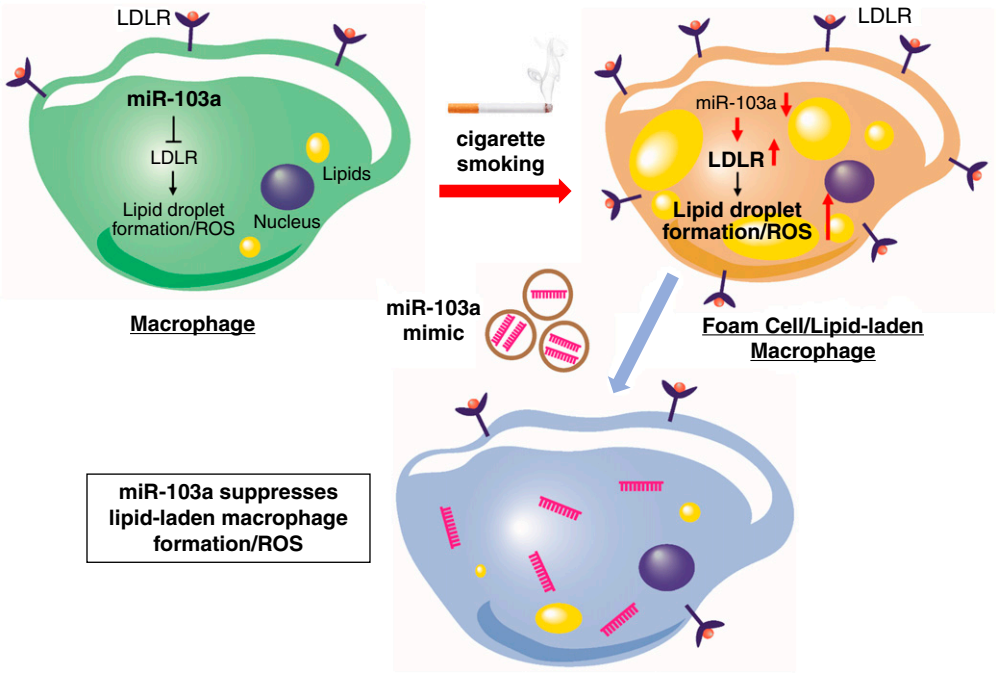

Figure 7. Schematic review of CS-induced lipid-laden macrophage formation mediated by downregulation of miR-103a. In macrophages, miR-103a directly targets LDLR, which modulates lipid uptake and droplet formation. In response to CS exposure, miR-103a is downregulated by a high ROS level. In contrast, the elevated LDLR caused by reduced miR-103 promotes lipid-laden macrophage formation and increases intracellular ROS levels. Overexpression of miR-103a suppresses CS-induced lipid droplet accumulation and increases intracellular ROS levels, suggesting that miR-103a plays a critical role in altering lipid metabolism in macrophages.

increased accumulation of intracellular lipids and ROS levels (Figure 7). The latter may perpetuate or amplify the reduced cellular expression of miR-103a and lipid accumulation in macrophages, as increased oxidative stress levels in macrophages have been reported to induce changes in their lipid metabolism (40, 41).

Our study has several limitations. Further investigation is needed to assess whether miR-103a suppresses lipid-laden macrophage formation by reducing macrophage ROS production. In addition, all the functional studies were performed using the gain-of-function approaches by transfecting miR-103a mimic. Although a miR-103a inhibitor was used in our experiments, most of the observations were modest in magnitude or not statistically significant. However, in humans, the miR-103 family comprises three miRNAs: miR-103a, miR-103b, and miR-107, which share the same seed sequence (42). Thus, it is likely that miR-103a knockdown alone is insufficient to increase LDLR expression because of the persistence of miR-103b and miR-107. Nevertheless, in the setting of COPD and CS exposure, miR-103a levels in lung macrophages are downregulated, and overexpressing miR-103a is sufficient to reduce LDLR expression, lipid accumulation, and intracellular oxidative stress levels in macrophages, suggesting that strategies to deliver exogenous miR-103a to the COPD lung may have therapeutic potential in COPD.

Conclusions

We identified a novel role for miR-103a in attenuating the lipid uptake in macrophages by reducing LDLR expression and inhibiting both mitochondrial and cellular ROS levels that are induced by the increases in oxidative stress that are associated with exposure of cells to CS. Most importantly, these findings reveal miR-103a augmentation as a novel therapeutic potential for CS-induced diseases such as COPD by suppressing ROS production by macrophages and the formation of lipid-laden macrophages. ■

Author disclosures are available with the text of this article at www.atsjournals.org.

Acknowledgment: The authors thank Katherine Hardwick (Clinical and Administrative Pharmacy, College of Pharmacy, University of Georgia) for her administrative support.

References

1. Barnes PJ, Burney PG, Silverman EK, Celli BR, Vestbo J, Wedzicha JA, *et al.* Chronic obstructive pulmonary disease. *Nat Rev Dis Primers* 2015;1:15076.
2. Barnes PJ. Oxidative stress-based therapeutics in COPD. *Redox Biol* 2020;33:101544.
3. Gershon AS, Warner L, Cascagnette P, Victor JC, To T. Lifetime risk of developing chronic obstructive pulmonary disease: a longitudinal population study. *Lancet* 2011;378:991–996.
4. Yawn B, Mannino D, Littlejohn T, Ruoff G, Emmett A, Raphiou I, *et al.* Prevalence of COPD among symptomatic patients in a primary care setting. *Curr Med Res Opin* 2009;25:2671–2677.

5. Lugg ST, Scott A, Parekh D, Naidu B, Thickett DR. Cigarette smoke exposure and alveolar macrophages: mechanisms for lung disease. *Thorax* 2022;77:94–101.
6. Bahr TM, Hughes GJ, Armstrong M, Reisdorph R, Coldren CD, Edwards MG, *et al.* Peripheral blood mononuclear cell gene expression in chronic obstructive pulmonary disease. *Am J Respir Cell Mol Biol* 2013;49: 316–323.
7. Decramer M, Janssens W, Miravitlles M. Chronic obstructive pulmonary disease. *Lancet* 2012;379:1341–1351.
8. Morissette MC, Lamontagne M, Bérubé JC, Gaschler G, Williams A, Yauk C, *et al.* Impact of cigarette smoke on the human and mouse lungs: a gene-expression comparison study. *PLoS One* 2014;9:e92498.
9. Botelho FM, Gaschler GJ, Kianpour S, Zavitz CC, Trimble NJ, Nikota JK, *et al.* Innate immune processes are sufficient for driving cigarette smoke-induced inflammation in mice. *Am J Respir Cell Mol Biol* 2010; 42:394–403.
10. Hu Z, Xiao D, Qiu T, Li J, Liu Z. Microrna-103a curtails the stemness of non-small cell lung cancer cells by binding otub1 via the hippo signaling pathway. *Technol Cancer Res Treat* 2020;19:1533033820971643.
11. Telenga ED, Hoffmann RF, Ruben t'Kindt, Hoonhorst SJ, Willemse BW, van Oosterhout AJ, *et al.* Untargeted lipidomic analysis in chronic obstructive pulmonary disease. Uncovering sphingolipids. *Am J Respir Crit Care Med* 2014;190:155–164.
12. Hwang HW, Mendell JT. MicroRNAs in cell proliferation, cell death, and tumorigenesis. *Br J Cancer* 2006;94:776–780.
13. Ling H, Fabbri M, Calin GA. MicroRNAs and other non-coding RNAs as targets for anticancer drug development. *Nat Rev Drug Discov* 2013; 12:847–865.
14. Dutta RK, Chinnapaiyan S, Unwalla H. Aberrant micrornaomics in pulmonary complications: implications in lung health and diseases. *Mol Ther Nucleic Acids* 2019;18:413–431.
15. Mei D, Tan WSD, Tay Y, Mukhopadhyay A, Wong WSF. Therapeutic RNA strategies for chronic obstructive pulmonary disease. *Trends Pharmacol Sci* 2020;41:475–486.
16. Wang X, Zhang D, Higham A, Wolosianka S, Gai X, Zhou L, *et al.* ADAM15 expression is increased in lung $CD8^+$ T cells, macrophages, and bronchial epithelial cells in patients with COPD and is inversely related to airflow obstruction. *Respir Res* 2020;21:188.
17. Nielsen TB, Yan J, Luna B, Spellberg B. Murine oropharyngeal aspiration model of ventilator-associated and hospital-acquired bacterial pneumonia. *J Vis Exp* 2018;136:57672.
18. Nayak DK, Mendez O, Bowen S, Mohanakumar T. Isolation and in vitro culture of murine and human alveolar macrophages. *J Vis Exp* 2018; 134:57287.
19. Fan Z, Yang J, Zhang D, Zhang X, Ma X, Kang L, *et al.* The risk variant rs884225 within EGFR impairs miR-103a-3p's anti-tumourigenic function in non-small cell lung cancer. *Oncogene* 2019;38:2291–2304.
20. Abugessaisa I, Shimoji H, Sahin S, Kondo A, Harshbarger J, Lizio M, *et al.*; FANTOM consortium. Fantom5 transcriptome catalog of cellular states based on semantic mediawiki. *Database (Oxford)* 2016;2016: baw105.
21. Morsch ALBC, Wisniewski E, Luciano TF, Comin VH, Silveira GB, Marques SO, *et al.* Cigarette smoke exposure induces ROS-mediated autophagy by regulating sestrin, AMPK, and mTOR level in mice. *Redox Rep* 2019;24:27–33.
22. Yan J, Horng T. Lipid metabolism in regulation of macrophage functions. *Trends Cell Biol* 2020;30:979–989.
23. Poliska S, Csanky E, Szanto A, Szatmari I, Mesko B, Szeles L, *et al.* Chronic obstructive pulmonary disease-specific gene expression signatures of alveolar macrophages as well as peripheral blood monocytes overlap and correlate with lung function. *Respiration* 2011; 81:499–510.
24. Dewhurst JA, Lea S, Hardaker E, Dungwa JV, Ravi AK, Singh D. Characterisation of lung macrophage subpopulations in COPD patients and controls. *Sci Rep* 2017;7:7143.
25. Morissette MC, Shen P, Thayaparan D, Stämpfli MR. Disruption of pulmonary lipid homeostasis drives cigarette smoke-induced lung inflammation in mice. *Eur Respir J* 2015;46:1451–1460.
26. Canton M, Sánchez-Rodríguez R, Spera I, Venegas FC, Favia M, Viola A, *et al.* Reactive oxygen species in macrophages: sources and targets. *Front Immunol* 2021;12:734229.
27. Jiménez-Ruiz CA, Andreas S, Lewis KE, Tonnesen P, van Schayck CP, Hajek P, *et al.* Statement on smoking cessation in COPD and other pulmonary diseases and in smokers with comorbidities who find it difficult to quit. *Eur Respir J* 2015;46:61–79.
28. Garcia-Aymerich J, Lange P, Benet M, Schnohr P, Antó JM. Regular physical activity reduces hospital admission and mortality in chronic obstructive pulmonary disease: a population based cohort study. *Thorax* 2006;61:772–778.
29. Taylor AE, Finney-Hayward TK, Quint JK, Thomas CM, Tudhope SJ, Wedzicha JA, *et al.* Defective macrophage phagocytosis of bacteria in COPD. *Eur Respir J* 2010;35:1039–1047.
30. Madison MC, Landers CT, Gu BH, Chang CY, Tung HY, You R, *et al.* Electronic cigarettes disrupt lung lipid homeostasis and innate immunity independent of nicotine. *J Clin Invest* 2019;129:4290–4304.
31. Sun Z, Zhang Q, Yuan W, Li X, Chen C, Guo Y, *et al.* MiR-103a-3p promotes tumour glycolysis in colorectal cancer via hippo/YAP1/HIF1A axis. *J Exp Clin Cancer Res* 2020;39:250.
32. Liang J, Liu X, Xue H, Qiu B, Wei B, Sun K. MicroRNA-103a inhibits gastric cancer cell proliferation, migration and invasion by targeting c-Myb. *Cell Prolif* 2015;48:78–85.
33. Olemukan RE, Eller LA, Ouma BJ, Etonu B, Erima S, Naluyima P, *et al.* Quality monitoring of HIV-1-infected and uninfected peripheral blood mononuclear cell samples in a resource-limited setting. *Clin Vaccine Immunol* 2010;17:910–918.
34. Patel KM, Strong A, Tohyama J, Jin X, Morales CR, Billheimer J, *et al.* Macrophage sortilin promotes LDL uptake, foam cell formation, and atherosclerosis. *Circ Res* 2015;116:789–796.
35. Steinberg D. The LDL modification hypothesis of atherogenesis: an update. *J Lipid Res* 2009;50:S376–S381.
36. Linton MF, Babaev VR, Gleaves LA, Fazio S. A direct role for the macrophage low density lipoprotein receptor in atherosclerotic lesion formation. *J Biol Chem* 1999;274:19204–19210.
37. Yao H, Rahman I. Current concepts on oxidative/carbonyl stress, inflammation and epigenetics in pathogenesis of chronic obstructive pulmonary disease. *Toxicol Appl Pharmacol* 2011;254:72–85.
38. Xu MC, Gao XF, Ruan C, Ge ZR, Lu JD, Zhang JJ, *et al.* Mir-103 regulates oxidative stress by targeting the bcl2/adenovirus e1b 19 kda interacting protein 3 in huvecs. *Oxid Med Cell Longev* 2015;2015:489647.
39. Li J, He W, Wang Y, Zhao J, Zhao X. miR-103a-3p alleviates oxidative stress, apoptosis, and immune disorder in oxygen-glucose deprivation-treated BV2 microglial cells and rats with cerebral ischemia-reperfusion injury by targeting high mobility group box 1. *Ann Transl Med* 2020; 8:1296.
40. Seo E, Kang H, Choi H, Choi W, Jun HS. Reactive oxygen species-induced changes in glucose and lipid metabolism contribute to the accumulation of cholesterol in the liver during aging. *Aging Cell* 2019; 18:e12895.
41. Jin Y, Tan Y, Chen L, Liu Y, Ren Z. Reactive oxygen species induces lipid droplet accumulation in hepg2 cells by increasing perilipin 2 expression. *Int J Mol Sci* 2018;19:3445.
42. Ideozu JE, Zhang X, Rangaraj V, McColley S, Levy H. Microarray profiling identifies extracellular circulating miRNAs dysregulated in cystic fibrosis. *Sci Rep* 2019;9:15483.